Polymer Chemistry

ROYAL SOCIETY OF CHEMISTRY

PAPER

View Article Online
View Journal | View Issue

Cite this: *Polym. Chem.*, 2020, **11**, 7354

Analysis of cyclic polymer purity by size exclusion chromatography: a model system†

Yanlin Shi, Sung-Po R. Chen, Zhongfan Jia ‡ and Michael J. Monteiro *

Received 6th September 2020,
Accepted 27th October 2020

DOI: 10.1039/d0py01277g

rsc.li/polymers

Because cyclic polymers have intriguing physical properties, considerable synthetic strategies have been developed to create a wide variety of cyclic architectures. One of the most utilized cyclization procedures is *via* ring-closure of a difunctional linear polymer using the copper catalyzed azide–alkyne cycloaddition (CuAAC) 'click' reaction. However, quantifying the percentage of mono-cyclic species (*i.e.* formed directly from the starting α,ω-linear polymer) still remains a challenge even with access to a variety of characterization techniques, including NMR, MALDI-ToF, size exclusion chromatography (SEC) and liquid chromatography at the critical condition (LCCC). Here, we demonstrated that SEC in combination with the log-normal distribution (LND) method and minimization of the sum of squares of the weighted residuals to fit the distribution provided an analytical method for the accurate analysis of cyclic purity. The key to the SEC analysis method relies on quantification of the hydrodynamic shift from linear to mono-cyclic. The technique developed in this work has wide applicability for the characterization of complex polymer architectures and compositions (and can be easily applied to sequence controlled polymers).

Introduction

The unique physical properties of cyclic polymers in bulk and solution make simple and complex cyclic topologies of significant interest across many disciplines of science.[1,2] A lack of chain ends and a more compact configuration significantly improves the stability of biological cyclic macromolecules, including peptides, proteins and DNA, against enzymatic degradation and denaturation.[3] Many highly potent toxins in nature have cyclic topological constituents (*e.g.*, venom from the black mamba snake has an LD50 subcutaneous of 0.32 mg kg^{-1}, which can kill humans in less than 30 min[4]). It is, therefore, not surprising that therapeutic companies synthesize cyclic peptides and proteins for better pharmacological outcomes. For example, the copper catalyzed azide–alkyne cycloaddition (CuAAC) reaction to cyclize hairpin decoy oligonucleotides produced greater enzymatic stability and enhanced cell uptake.[5] When applying cyclic polymers to non-biological applications, Kapnistos *et al.*[6] showed in a seminal paper that the viscoelastic properties in the melt of cyclic polystyrene in its 'pure' form (*i.e.*, "as pure as currently possible") showed no plateau modulus. It was postulated that the complex dynamics of the double-folded cyclic loops could be described by the lattice-animal model. More importantly, doping the 'pure' cyclic with even a small amount of linear impurity (volume fraction of 0.0007) significantly influenced the viscoelastic properties to have similar properties to that of the linear polymer. Liquid chromatography at the critical condition (LCCC)[7–12] was used to purify their cyclic polymers of high molecular weights (*i.e.* 161 000 g mol^{-1} and 198 000 g mol^{-1}), and showed excellent separation and resolution between linear and cyclic polystyrene at high molecular weights.

In recent years, the CuAAC coupling reaction has produced low molecular weight cyclic polymers *via* the ring closure method.[1,13] Low molecular weight α,ω-functionalized linear polymers are more amenable to cyclization as quantitatively described by the Jacobson-Stockmayer equation,[14,15] in which the probability of cyclization decreases with the power law dependence of −3/2 with increasing chain length. Our group has further elaborated on this method, creating a wide variety of complex topologies made from cyclic polymer building blocks,[15–20] and their physical properties examined both in solution and bulk.[21–23] With the ever increasing use of the CuAAC 'click' reaction to produce a variety of cyclic polymers *via* the ring closure method, purity of the resultant cyclic becomes critically important. The ring closure method, depending upon the reaction conditions, will produce the desired mono-cyclic species (consisting of only one triazol ring in the cyclic) and the additional undesired starting linear,

Australian Institute for Bioengineering and Nanotechnology, The University of Queensland, Brisbane QLD 4072, Australia. E-mail: m.monteiro@uq.edu.au

†Electronic supplementary information (ESI) available: Computer code to distribution fitting. See DOI: 10.1039/d0py01277g

‡Current address: College of Science and Engineering, Flinders University, Sturt Road, Bedford Park, South Australia 5042, Australia

linear and cyclic multiblocks (*i.e.* multiple triazols in the cyclic) polymer species.[15,24] The main methods to characterize these species are size exclusion chromatography (SEC), MALDI-ToF, NMR, and in a few cases LCCC. Each characterization tool has its limitations.[25–27] The LCCC method requires non-trivial optimization of the conditions, and at molecular weights of less than 10 000 g mol^{-1} found not to be satisfactory for the quantitation of cyclic polystyrene based on the critical adsorption point (CAP) of linear precursors.[12,28] When using the CAP for cyclic polymer, however, good resolution and cyclic purity were found.[28] It was noted that linear species with higher molecular weights after the CuAAC reaction interfere with the LCCC analysis regardless of which CAP method was used as these lie between the starting linear and mono-cyclic polymer peaks, and thus need to be minimized.

The universally used analysis technique by researchers for the characterization of cyclic polymers is SEC due to the clear and observable shift in the molecular weight distribution (MWD) from linear to cyclic when using only the refractive index detector. SEC is also readily available in most if not all polymer laboratories and is quite straightforward to derive molecular weight distribution data. The disadvantage of SEC for quantifying cyclic polymer is the significant overlap in the SEC chromatograms with linear species, and hence the difficulty in determining cyclic purity. One advantage of SEC is that all higher molecular weight linear and cyclic multiblocks do not interfere with the mono-cyclic distribution. In our own work, we quantified the amounts of mono-cyclic to other species by fitting (or deconvolution of) the MWD from SEC by analysis using the log-normal distribution (LND) model.[29] This procedure allowed quantification of the weight fractions of all (or most) species in the polymer MWD after ring closure. We found that the peak molecular weight (M_p) of the cyclic was 0.76 times less than that of the M_p of the linear polymer using refractive index and a polystyrene calibration curve.[19] The fitting procedure used visual inspection of the fit to the experimental MWD by changing the weight fraction of each possible species. Although visualization gave satisfactory results, removing this visual subjectivity would provide greater accuracy. To accomplish this, we use here a simple method based on minimizing the sum of squares of the weighted residuals to determine the relative weight fractions of polymer species. Cyclization of an α,ω-functionalized linear polystyrene (l-PSTY) with an alkyne and azide end-groups, using the Cu-catalyzed azide/alkyne cycloaddition (CuAAC) reaction, produced a mono-cyclic polystyrene (c-PSTY) as shown in Scheme 1.[15] The sensitivity and accuracy of SEC/LND method was determined by doping the cyclic non-purified polymer after the 'click' reaction with different amounts of linear starting polymer (l-PSTY). The work presented here validated the accuracy of the SEC/LND method for low molecular weight cyclic polymers in the absence of other direct characterization techniques, and suggests the applicability of this technique to characterization of precision-made complex polymer architectures[30,31] and sequence controlled polymers.[32]

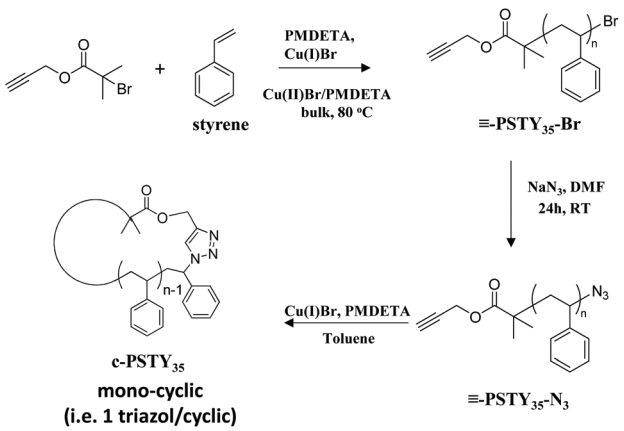

Scheme 1 Synthetic route for the cyclization of polystyrene (c-PSTY).

Experimental

Materials

The following reagents were used as received: alumina, activated basic (Aldrich: Brockmann I, standard grade, ~150 mesh, 58 Å), magnesium sulfate, anhydrous ($MgSO_4$: Scharlau, extra pure), copper(II)bromide (Aldrich, 99%), silica gel 60 (230–400 mesh ATM (SDS)), sodium hydrogen carbonate (Merck, AR grade), triethylamine (TEA: Fluka, 98%), 2-bromo-2-methylpropionyl bromide (Aldrich, 98%), propargyl alcohol (Aldrich, 99%), PMDETA (Aldrich, 99%), sodium azide (NaN_3: Aldrich, ≥99.5%), TLC plates (silica gel 60 F254). Styrene (Aldrich, >99%) was passed through a basic alumina column to remove inhibitor, and then used in the polymerizations.

Nuclear magnetic resonance (NMR)

All NMR spectra were recorded on a Bruker DRX 400 MHz spectrometer using an external lock ($CDCl_3$) and referenced to the residual nondeuterated solvent ($CHCl_3$).

Size exclusion chromatography (SEC)

All polymer samples were dried prior to analysis in a vacuum oven at 50 °C for 24 h. The dried polymer was dissolved in tetrahydrofuran (THF) to a concentration of ~20 mg mL^{-1} and then filtered through a 0.45 μm PTFE syringe filter. Analysis of the molecular weight distributions of the polymers was accomplished using a Waters 2695 separations module, fitted with a Waters 410 refractive index detector maintained at 35 °C, a Waters 996 photodiode array detector, and two Ultrastyragel linear columns (7.8 × 300 mm) arranged in series. These columns were maintained at 40 °C for all analyses and are capable of separating polymers in the molecular weight range of 500–4 million g mol^{-1} with high resolution. All samples were eluted at a flow rate of 1.0 mL min^{-1}. Calibration was performed using narrow molecular weight PSTY standards ($Đ \leq 1.1$) ranging from 500 to 2 million g mol^{-1}. Data acquisition was performed using Empower software, and molecular weights were calculated relative to polystyrene standards.

Attenuated total reflectance-Fourier transform spectroscopy (ATR-FTIR)

ATR-FTIR spectra were obtained using a horizontal, single bounce, diamond ATR accessory on a Nicolet Nexus 870 FT-IR. Spectra were recorded between 4000 and 500 cm^{-1} for 128 scans. Solids were pressed directly onto the diamond internal reflection element of the ATR without further sample preparation.

Synthesis of $CuBr_2$/PMDETA complex

Copper(II)bromide ($CuBr_2$, 4.1 g, 1.84×10^{-2} mol) was stirred in MeOH (200 mL) until complete dissolution was achieved. PMDETA (3.2 g, 1.85×10^{-2}) was added dropwise to this solution, and then stirred for an additional 60 min at room temperature. The reaction mixture was concentrated to ~30 mL, and 20 mL of diethyl ether was added to the solution at which point the complex started to precipitate. The precipitated complex was collected by vacuum filtration, washed with diethyl ether and dried in a vacuum for 24 h at 25 °C.

Synthesis of propargyl 2-bromoisobutyrate (initiator)

2-Bromo-2-methylpropionyl bromide (6.61 mL, 53.48 mmol) dissolved in DCM (50 mL) at room temperature was added dropwise to a stirred solution of propargyl alcohol (2.08 mL, 35.67 mmol) and TEA (8 mL) in DCM (100 mL) at 0 °C. This reaction mixture was stirred at room temperature overnight. The resulting solution was washed with saturated aqueous $NaHCO_3$ and brine, dried over $MgSO_4$, filtered, and concentrated by rotary-evaporation. The resulting material was purified by a silica chromatography with petroleum spirit/ethyl acetate (10/1, v/v) as the eluent to obtain propargyl 2-bromoisobutyrate as a clear, colorless oil (yield = 75.28%, 5.13 g, 28.86 mmol). ^{1}H NMR ($CDCl_3$, 298 K, 400 MHz): δ 4.76 (d, 2H, J = 2.48 Hz, CH_2O), 2.50 (t, 1H, J = 2.40 Hz, C≡CH), and 1.95 (s, 6H, $(CH_3)_2C$). ^{13}C NMR ($CDCl_3$, 298 K, 400 MHz): 170.9, 76.9, 75.4, 54.9, 53.4, 30.6.

Synthesis of ≡-$PSTY_{35}$-Br

The $CuBr_2$/PMDETA complex (77.05 mg, 0.19 mmol), styrene (9.13 g, 87.71 mmol), PMDETA (0.203 mL, 0.97 mmol), and initiator (199.92 mg, 0.97 mmol) were added to a 50 mL Schlenk flask equipped with a magnetic stirrer, and then purged with argon for 30 min to remove oxygen. Cu(I)Br (138.64 mg, 0.97 mmol) was added to the polymerization mixture above under an argon blanket, degassed for a further 5 min, and placed into a temperature-controlled oil bath at 80 °C. A sample was taken at approximately 4 h to determine conversion; if conversion was close to 50%, the polymerization mixture quenched in an ice bath and diluted with $CHCl_3$ (at ~3 fold to the reaction mixture volume). The reaction could be left longer, if required, to reach ~50% conversion. To the polymer solution, neutral Al_2O_3 (~1.5 g) was added to complex with copper salts under Argon, and the mixture passed through an activated neutral alumina column. The resultant solution was concentrated by rotary-evaporation, the polymer recovered by precipitation into a large volume of MeOH (~20-fold excess to polymer solution), and vacuum filtration. The polymer without drying was used directly in the next azidation step. A fraction of this polymer (~0.2 g) was dried in a vacuum at 25 °C for 10 h to obtain a white powder for NMR and SEC characterization (M_n = 3670 and $Đ$ = 1.11 based on a PSTY calibration curve).

Synthesis of ≡-$PSTY_{35}$-N_3

The polymer (≡-$PSTY_{35}$-Br), with a mass based on conversion, was dissolved in DMF (40 mL) and NaN_3 (1.10 g, 19.6 mmol, ~20 equiv. to initiator) under Argon at 25 °C for 24 h. The reaction solution was concentrated by an airflow to approximately a third of its original volume, precipitated into MeOH (20-fold excess to polymer solution), recovered by vacuum filtration, and washed with H_2O and MeOH. The azide polymer was dried *in vacuo* at 25 °C for 24 h to obtain a white powder (approximately 4 g), which was characterized by NMR and SEC (M_n = 3690 and $Đ$ = 1.10 based on a PSTY calibration curve).

Synthesis of c-$PSTY_{35}$

A degassed (30 min purging) solution of PMDETA (0.846 mL, 4.05 mmol) in 15 mL of dry toluene was added *via* a double tip needle to a dry Schlenk flask under argon containing CuBr (582.30 mg, 4.06 mmol) over a 5 min period. Formation of the CuBr/PMDETA complex was observed in the formation of a clear solution. To this solution, we added a solution of linear ≡-$PSTY_{35}$-N_3 (0.30 g, 0.08 mmol) in 15 mL of dry toluene *via* a syringe pump at a rate of 0.2 mL min^{-1}. After complete addition of the polymer solution (*i.e.* 70 min), the reaction mixture was stirred for a further 3 h. Toluene was evaporated from the solution using an airflow, the remaining polymer was dissolved in DCM, and passed through an activated basic alumina column. The polymer was recovered by precipitation into MeOH (20-fold excess to polymer solution) and then filtered with the aid of a vacuum. The polymer was dried under vacuum at 25 °C for 24 h, resulting in the crude cyclic polymer (~0.27 g) as white powder (M_n = 2950, $Đ$ = 1.26 based on PSTY calibration curve).

Results and discussion

An in-depth analysis of the SEC chromatograms can be used to determine the purity of the cyclic polymer; a methodology used by our group in a quantitative manner to provide evidence for cyclic formation. Intuitively, a decrease in the apparent M_w (or decrease in hydrodynamic volume) may suggest high cyclic purity, but the absolute change (or $M_{p,cyclic}/M_{p,linear}$) from pure linear to pure cyclic is the key parameter to quantify the amount of cyclic after ring closure. This value can be determined from the change in the peak molecular weight M_p when using the weight distribution (*i.e.* $w(M)$), and was found that after CuAAC cyclization and purification by preparative SEC was $M_{p,cyclic} = 0.76\ M_{p,linear}$.[19] Here, the CuAAC cyclization method to produce c-PSTY showed a clear shift in hydrodynamic volume in the SEC traces using a refractive index detector and a linear polystyrene calibration curve (Fig. 1). The resultant cyclic product was not further purified. First, l-PSTY

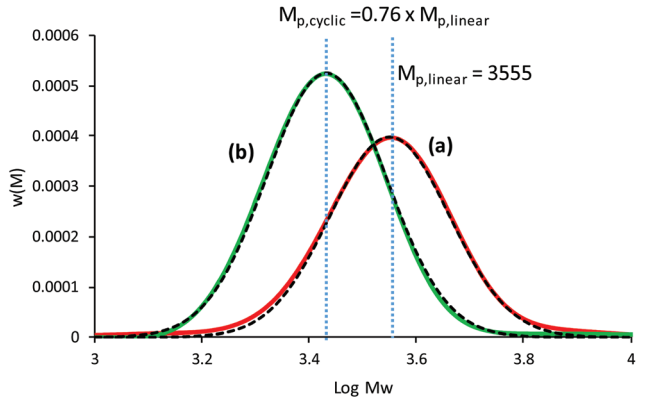

Fig. 1 SEC chromatograms of the cyclization of linear $PSTY_{35}$. (A) before, and (B) after CuAAC coupling reaction. Dashed lines represent the fit using the LND method using for linear M_n = 3674 and $Đ$ = 1.068. The cyclic polymer was fit using $M_{p,cyclic}$ = 0.76 $M_{p,linear}$ (*i.e.* M_n = 2799, $Đ$ = 1.068).

(red solid line) was analyzed by the LND method (dotted curve), and the best fit with a Gaussian distribution was using an M_n of 3674 and dispersity index ($Đ$) of 1.068. The purity of difunctional l-PSTY that would lead exclusively to mono-cyclic c-PSTY was 93.5%, with the other 6.5% consisting of high molecular cyclic or linear polymers. Using the value of 0.76 for the shift in molecular weight, the fit of the cyclic product with a Gaussian distribution was excellent (M_n = 2799, $Đ$ = 1.068) with a purity of 94%, no linear starting material and only 6% higher molecular weight polymer species. This data suggests that our cyclization procedure was near quantitative.

We demonstrate that the SEC/LND method[29,33] is quite powerful to determine the weight fraction of linear in the cyclic product. A theoretical MWD simulated using the LND method and an M_p shift of 0.76 for a variety of linear and cyclic mixtures was shown in Fig. 2A. No matter the weight fraction of c-PSTY ($w_{cyclic;}$ from 0.25, 0.5 and 0.75), we observed no separation between the linear and cyclic MWDs; that is, all distributions were monomodal. To determine the M_n and $Đ$ of these mixtures we used the method of moments. The generalized equation for the different moments is as follows:

$$\mu_i \equiv \sum_{r=0}^{\infty} r^i [P_r] \quad (1)$$

where μ is the moment, i is the moment order (*i.e.* zeroth, first order, second order...), r is the chainlength of the polymer, and P_r is the concentration of polymer chains at chainlength r. It can be seen that the zeroth moment (i = 0) represents the concentration of polymer chains of the whole distribution, and the first moment (i = 0) represents the concentration of monomer units within the polymer. Calculation of the first three moment orders allows the number-average (M_n) and weight average (M_w) of the MWD as shown below.

$$M_n \equiv \frac{\mu_1}{\mu_0} M_{w,mon} \quad (2)$$

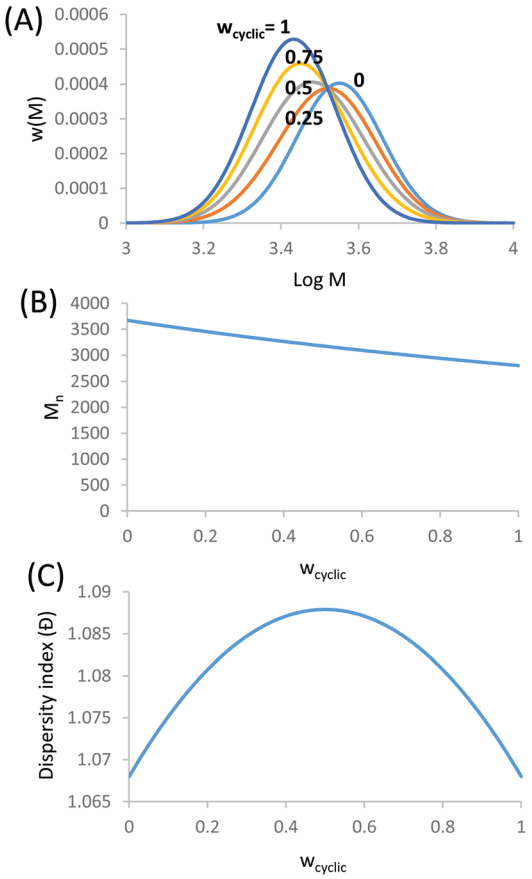

Fig. 2 Theoretical mixture of linear and cyclic distributions. (A) SEC distributions using the M_n and $Đ$ for linear and cyclic from Fig. 1. (B) M_n for the mixture of linear and cyclic determined from the method-of-moments. (C) $Đ$ for the mixture of linear and cyclic determined from the method-of-moments. Where w_{cyclic} is the weight fraction of cyclic to linear.

$$M_w \equiv \frac{\mu_2}{\mu_1} M_{w,mon} \quad (3)$$

$$\equiv \frac{M_w}{M_n} = \frac{\mu_0 \mu_2}{(\mu_1)^2} \quad (4)$$

To add two different MWDs, we can use the above equations to determine the moment order of each distribution since the M_n and M_w of each distribution and its concentration within the total MWD (*i.e.* both distributions added together) are known:

$$M_{n,total} = \frac{\mu_{1,D1} + \mu_{1,D2}}{\mu_{0,D1} + \mu_{0,D2}} M_{w,mon} \quad (5)$$

$$M_{w,total} = \frac{\mu_{2,D1} + \mu_{2,D2}}{\mu_{1,D1} + \mu_{1,D2}} M_{w,mon} \quad (6)$$

where $D1$ and $D2$ represents distributions 1 and 2.

The addition of the linear (M_n = 3674, $Đ$ = 1.068) and cyclic (M_n = 2799, $Đ$ = 1.068) MWDs using the method of moments at varying ratios of linear to cyclic showed a linear decrease in M_n

as the weight fraction of cyclic increased (Fig. 2B). In a real MWD system, which usually contains high molecular weight species, such an analysis would lead to large errors. A more subtle method to discriminate between the two MWDs may be observed from a change in the dispersity index. As observed in Fig. 2C, $Đ$ increased to a maximum at weight fraction of 0.5, and then decreased to a value of $Đ$ of the pure cyclic polymer. Thus, although the MWDs from Fig. 2A were all monomodal, the subtle change in both the M_n and $Đ$ of these mixtures provided some insight into determining the ratio of linear to cyclic. This has been long neglected in previous work, relying only on an observable shift in elution volume (or time) to justify cyclic formation.[34–38] As shown above, much of the cyclic polymer synthesized in the literature may possibly include large amounts of starting linear or other polymer species. This finding may also apply to characterization of other complex topologically and compositionally different polymers.

In testing the accuracy of the SEC/LND method, we used the linear and cyclic described above as a model system. The weight fractions of cyclic was experimentally determined from the addition of stock solutions of linear and cyclic polymers (see Table 1). Care was taken in pipetting in the various ratios of solutions, but it should be noted that errors can arise due to instrumental error from the balance, pipette and even evaporation of THF from the stock solutions. A simple method to determine the true weight fraction of cyclic was to add the MWDs of the c-PSTY and l-PSTY and match this to the experimental MWD at a specific weight fraction of each polymer species. To find the optimal weight fraction, we minimized the residual sum of squares (ss)[39] between the fit and experimental MWDs using a computer program (see ESI for the computer code†). The sum of the data points of the ss was determined as follows:

$$\mathrm{ss}\left(w_{\mathrm{cyclic}}, w(M)\right) = \sum_{M_{w=0}}^{n} \left(w(M)_{\exp t, M_w} - w(M)_{\mathrm{fit}, M_w} \right)^2 \quad (7)$$

where w_{cyclic} is the weight fraction of cyclic (and $w_{\mathrm{linear}} = 1 - w_{\mathrm{cyclic}}$), $w(M)$ is the intensity of the weight-average MWD at M. The computer code used very small step sizes of 0.001 for w_{cyclic} from 0 to 1. To account for any base line drift in the SEC, we also included a scaling factor to provide the best fit especially at the peak maximum.

The simulated fit using the cyclic weight fraction determined from the residual sum of squares matched to all the experimental SEC chromatograms (see Fig. 3, which showed selected distributions covering a range of w_{cyclic}). The fit at the peak of the distribution was also in good agreement with the experimental SEC traces, with the peak max approaching that of the pure cyclic at higher weight fractions. This fit provided the true weight fraction of l-PSTY doped into c-PSTY and was found to be slightly different to the targeted values due to the associated instrumental error. Regardless, the fitting of the two distributions provided a better and more accurate method to determine the ratio of linear to cyclic. It should be noted that w_{cyclic} determined in this case was for the full distribution of both linear and cyclic, including the high molecular weight species.

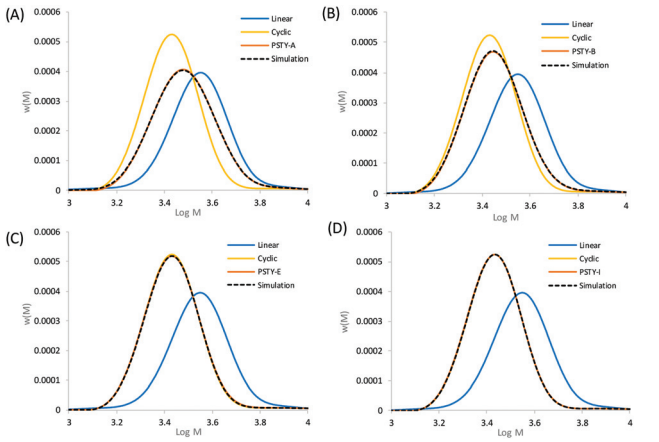

Fig. 3 Experimental SEC traces of mixtures of linear and cyclic (see Table 1). (A) PSTY-A with targeted w_{cyclic} = 49.72%, (B) PSTY-B with targeted w_{cyclic} = 77.96%, (C) PSTY-E with targeted w_{cyclic} = 95.68%, and (D) PSTY-I with targeted w_{cyclic} = 99.50%. The dashed lines are the fit using the ss to determine w_{cyclic} calculated from fitting the experimental linear and cyclic distributions to the experimental distribution.

Table 1 Stock solutions used to prepare cyclic and linear polymer at targeted ratios and the fits to experimental data and the SEC/LND model

Polymer	Linear			Cyclic			Cyclic (wt%)			
	Stock solution (mg mL^{-1})	V_{THF} (μL)	Mass$_{\mathrm{linear}}$ (mg)	Stock solution (mg mL^{-1})	V_{THF} (μL)	Mass$_{\mathrm{cyclic}}$ (mg)	Target (%)	Expt.[a] (%)	Expt.[b](accounting for pure cyclic) (%)	LND fit[c] (%)
PSTY$_{35}$-A	4.378	200	0.9461	9.4612	100	0.9461	49.72	49.40	49.53	51.67
PSTY$_{35}$-B		80	0.3827		160	1.5138	79.82	77.87	77.96	80.93
PSTY$_{35}$-C		40	0.1913		180	1.7030	89.90	91.34	91.38	94.86
PSTY$_{35}$-D	1.0257	100	0.1026		190	1.7976	94.60	95.56	95.58	99.20
PSTY$_{35}$-E		80	0.0821		192	1.8166	95.68	98.58	98.59	100.00
PSTY$_{35}$-F		60	0.0615		194	1.8355	96.76	99.56	99.56	99.14
PSTY$_{35}$-G		40	0.0410		196	1.8544	97.84	99.95	99.95	98.42
PSTY$_{35}$-H	0.0939	200	0.0188		198	1.8733	99.01	96.41	96.43	97.63
PSTY$_{35}$-I		100	0.0094		199	1.8828	99.50	100.00	100.00	100.00
PSTY$_{35}$-J		50	0.0047		199.5	1.8875	99.75	98.41	98.42	99.63

[a] The experimental was determined by adding the cyclic and linear distributions and using the ss simulation. [b] The experimental distribution accounting for the amount of pure cyclic. [c] LND fit using the ss.

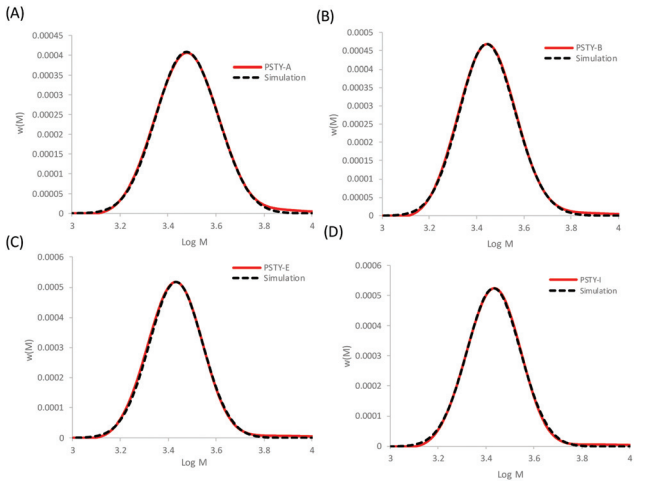

Fig. 4 Fitting the experimental linear and cyclic mixture with the individual linear and cyclic distributions found by ss and using the LND distributions in Fig. 1 (dashed lines). (A) PSTY-A with targeted w_{cyclic} = 49.72%, (B) PSTY-B with targeted w_{cyclic} = 77.96%, (C) PSTY-E with targeted w_{cyclic} = 95.68%, and (D) PSTY-I with targeted w_{cyclic} = 99.50%.

The Gaussian distributions for both the linear and cyclic polymers (as found from Fig. 1) were then used to find the optimal w_{cyclic} for the different ratios of doped linear (*i.e.* distributions A–J) using the residual sum of squares. This procedure was similar to the addition of the two distributions above. The fits using the LND method and the weight fraction determined by ss was excellent for all distributions (Fig. 4). As expected, the fit at high molecular weight ($M > 10^{3.8}$) was poor due to the high molecular weight species in both the linear and cyclic distributions. The weight fraction of pure cyclic found by the LND method was higher at lower weight fractions of cyclic and higher as the weight fraction approached 1. For distribution E, there was a non-quantifiable amount of linear (*i.e.* w_{cyclic} ~1). To compare the weight fraction values found by the LND method with those from the added distribution method (*i.e.* Fig. 3), the amount of non-pure linear and cyclic species was taken into account to determine the true weight fraction of pure linear and cyclic from the added distribution (see Table 1). It can be seen that there is still a small difference between the values from the LND and the added distribution methods as shown in Fig. 5. The difference was greatest at a weight fraction of ~0.5 (4%) and decreased to less than 2% with a further increase in w_{cyclic}. The data showed that SEC coupled with the LND method provided an accurate analysis of cyclic purity. We believe that the greater difference at intermediate weight fractions (*e.g.* 0.5–0.9) was most probably due to the increase in dispersity of the mixture (see Fig. 2C), and therefore a greater susceptible to minor baseline drifts in the SEC chromatograms.

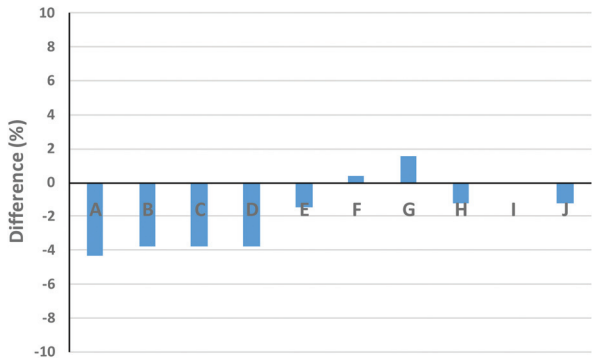

Fig. 5 Difference between the w_{cyclic} found from the experimental mixed distributions and w_{cyclic} from the LND (see Table 1).

Conclusions

In summary, the SEC/LND method successfully determined the amount of linear impurity after cyclization by the ring closure procedure. Using a polystyrene model system, we targeted varying ratios of linear to cyclic from stock solutions of c-PSTY and l-PSTY solutions. The mixtures were analyzed through the fit by ss and visualization of the fit from addition of two distributions using the found w_{cyclic}. The weight fraction of cyclic was different from that targeted but was similar to the values of w_{cyclic} found by the SEC/LND method. Taken together, the data supports that the use of the SEC coupled with the LND method provides an accurate and quantitative method to determine the amount of linear impurity in the cyclic. The key parameter of hydrodynamic shift is a requirement for the successful use of the SEC/LND method not only for polystyrene cyclic but all other low molecular weight polymers.

Conflicts of interest

There are no conflicts to declare.

Acknowledgements

The acknowledgements come at the end of an article after the conclusions and before the notes and references.

Notes and references

1 Z. F. Jia and M. J. Monteiro, Cyclic Polymers: Methods and Strategies, *J. Polym. Sci., Part A: Polym. Chem.*, 2012, **50**(11), 2085–2097.
2 F. M. Haque and S. M. Grayson, The synthesis, properties and potential applications of cyclic polymers, *Nat. Chem.*, 2020, **12**(5), 433–444.
3 D. J. Craik, N. L. Daly, T. Bond and C. Waine, Plant cyclotides: A unique family of cyclic and knotted proteins that defines the cyclic cystine knot structural motif, *J. Mol. Biol.*, 1999, **294**(5), 1327–1336.

4 D. J. Craik and C. I. Schroeder, Peptides from Mamba Venom as Pain Killers, *Angew. Chem., Int. Ed.*, 2013, **52**(11), 3071–3073.
5 A. H. El-Sagheer and T. Brown, Synthesis, Serum Stability and Cell Uptake of Cyclic and Hairpin Decoy Oligonucleotides for TCF/LEF and GLI Transcription Factors, *Int. J. Pept. Res. Ther.*, 2008, **14**(4), 367–372.
6 M. Kapnistos, M. Lang, D. Vlassopoulos, W. Pyckhout-Hintzen, D. Richter, D. Cho, T. Chang and M. Rubinstein, Unexpected power-law stress relaxation of entangled ring polymers, *Nat. Mater.*, 2008, **7**(12), 997–1002.
7 H. C. Lee, H. Lee, W. Lee, T. H. Chang and J. Roovers, Fractionation of cyclic polystyrene from linear precursor by HPLC at the chromatographic critical condition, *Macromolecules*, 2000, **33**(22), 8119–8121.
8 B. Lepoittevin, M.-A. Dourges, M. Masure, P. Hemery, K. Baran and H. Cramail, Synthesis and Characterization of Ring-Shaped Polystyrenes, *Macromolecules*, 2000, **33**(22), 8218–8224.
9 R. D. Adams and S. B. Falloon, The Catalytic Cyclooligomerization of Thietane by Trirhenium Cluster Complexes. A New Route to Polythiaether Macrocycles, *J. Am. Chem. Soc.*, 1994, **116**(23), 10540–10547.
10 S. E. Cabaniss, Q. H. Zhou, P. A. Maurice, Y. P. Chin and G. R. Aiken, A log-normal distribution model for the molecular weight of aquatic fulvic acids, *Environ. Sci. Technol.*, 2000, **34**(6), 1103–1109.
11 K. P. Chan, Y.-F. Wang, A. S. Hay, X. L. Hronowski and R. J. Cotter, Synthesis and Characterization of Novel Cyclic (Aryl Ether Ketone)s, Cyclic (Aryl Ether Phthalazine)s, and Cyclic (Aryl Ether Isoquinoline)s, *Macromolecules*, 1995, **28**(20), 6705–6717.
12 D. Cho, K. Masuoka, K. Koguchi, T. Asari, D. Kawaguchi, A. Takano and Y. Matsushita, Preparation and characterization of cyclic polystyrenes, *Polym. J.*, 2005, **37**(7), 506–511.
13 B. A. Laurent and S. M. Grayson, An efficient route to well-defined macrocyclic polymers via "Click" cyclization, *J. Am. Chem. Soc.*, 2006, **128**(13), 4238–4239.
14 H. Jacobson and W. H. Stockmayer, Intramolecular reaction in polycondensations. I. The theory of linear systems, *J. Chem. Phys.*, 1950, **18**, 1600–1606.
15 D. E. Lonsdale, C. A. Bell and M. J. Monteiro, Strategy for Rapid and High-Purity Monocyclic Polymers by CuAAC "Click" Reactions, *Macromolecules*, 2010, **43**(7), 3331–3339.
16 D. E. Lonsdale and M. J. Monteiro, Various polystyrene topologies built from tailored cyclic polystyrene via CuAAC reactions, *Chem. Commun.*, 2010, **46**(42), 7945–7947.
17 J. Kulis, Z. F. Jia and M. J. Monteiro, One-Pot Synthesis of Mikto Three-Arm AB(2) Stars Constructed from Linear and Macrocyclic Polymer Chains, *Macromolecules*, 2012, **45**(15), 5956–5966.
18 Z. F. Jia, D. E. Lonsdale, J. Kulis and M. J. Monteiro, Construction of a 3-Miktoarm Star from Cyclic Polymers, *ACS Macro Lett.*, 2012, **1**(6), 780–783.
19 M. D. Hossain, Z. F. Jia and M. J. Monteiro, Complex Polymer Topologies Built from Tailored Multifunctional Cyclic Polymers, *Macromolecules*, 2014, **47**(15), 4955–4970.
20 F. Amir, M. D. Hossain, Z. F. Jia and M. J. Monteiro, Precise grafting of macrocyclics and dendrons to a linear polymer chain, *Polym. Chem.*, 2016, **7**(43), 6598–6607.
21 M. D. Hossain, J. C. Reid, D. R. Lu, Z. F. Jia, D. J. Searles and M. J. Monteiro, Influence of Constraints within a Cyclic Polymer on Solution Properties, *Biomacromolecules*, 2018, **19**(2), 616–625.
22 A. Pipertzis, M. D. Hossain, M. J. Monteiro and G. Floudas, Segmental Dynamics in Multicyclic Polystyrenes, *Macromolecules*, 2018, **51**(4), 1488–1497.
23 Z. C. Yan, M. D. Hossain, M. J. Monteiro and D. Vlassopoulos, Viscoelastic Properties of Unentangled Multicyclic Polystyrenes, *Polymers*, 2018, **10**(9), 973–985.
24 D. E. Lonsdale and M. J. Monteiro, Kinetic Simulations for Cyclization of alpha,omega-Telechelic Polymers, *J. Polym. Sci., Part A: Polym. Chem.*, 2010, **48**(20), 4496–4503.
25 J. N. Hoskins, S. Trimpin and S. M. Grayson, Architectural Differentiation of Linear and Cyclic Polymeric Isomers by Ion Mobility Spectrometry-Mass Spectrometry, *Macromolecules*, 2011, **44**(17), 6915–6918.
26 A. M. Yol, D. Dabney, S. F. Wang, B. A. Laurent, M. D. Foster, R. P. Quirk, S. M. Grayson and C. Wesdemiotis, Differentiation of Linear and Cyclic Polymer Architectures by MALDI Tandem Mass Spectrometry (MALDI-MS2), *J. Am. Soc. Mass Spectrom.*, 2013, **24**(1), 74–82.
27 B. A. Laurent and S. M. Grayson, Synthetic approaches for the preparation of cyclic polymers, *Chem. Soc. Rev.*, 2009, **38**(8), 2202–2213.
28 L. F. Gao, J. Oh, Y. F. Tu and T. Chang, Preparation of low molecular weight cyclic polystyrenes with high purity via liquid chromatography at the critical condition, *Polymer*, 2018, **135**, 279–284.
29 M. J. Monteiro, Fitting molecular weight distributions using a log-normal distribution model, *Eur. Polym. J.*, 2015, **65**, 197–201.
30 M. Gavrilov, F. Amir, J. Kulis, M. D. Hossain, Z. F. Jia and M. J. Monteiro, Densely Packed Multicyclic Polymers, *ACS Macro Lett.*, 2017, **6**(9), 1036–1041.
31 M. N. Holerca, M. Peterca, B. E. Partridge, Q. Xiao, G. Lligadas, M. J. Monteiro and V. Percec, Monodisperse Macromolecules by Self-Interrupted Living Polymerization, *J. Am. Chem. Soc.*, 2020, **142**(36), 15265–15270.
32 F. Amir, Z. F. Jia and M. J. Monteiro, Sequence Control of Macromers via Iterative Sequential and Exponential Growth, *J. Am. Chem. Soc.*, 2016, **138**(51), 16600–16603.
33 M. J. Monteiro and M. Gavrilov, Characterization of heteroblock copolymers by the log-normal distribution model, *Polym. Chem.*, 2016, **7**(17), 2992–3002.
34 J. Zhao, Y. Zhou, Y. Zhou, N. Zhou, X. Pan, Z. Zhang and X. Zhu, A straightforward approach for the one-pot synthesis of cyclic polymers from RAFT polymers via thiol–Michael addition, *Polym. Chem.*, 2016, **7**(9), 1782–1791.

35 H. Shen and G. Wang, A versatile flash cyclization technique assisted by microreactor, *Polym. Chem.*, 2017, **8**(36), 5554–5560.
36 S. Zhang, X. Cheng, J. Wang, Z. Zhang, W. Zhang and X. Zhu, Synthesis of a cyclic-brush polymer with a high grafting density using activated ester chemistry via the "grafting onto" approach, *Polym. Chem.*, 2018, **9**(41), 5155–5163.
37 T. Yamamoto, S. Yagyu and Y. Tezuka, Light- and Heat-Triggered Reversible Linear-Cyclic Topological Conversion of Telechelic Polymers with Anthryl End Groups, *J. Am. Chem. Soc.*, 2016, **138**(11), 3904–3911.
38 M. A. Cortez, W. T. Godbey, Y. Fang, M. E. Payne, B. J. Cafferty, K. A. Kosakowska and S. M. Grayson, The Synthesis of Cyclic Poly(ethylene imine) and Exact Linear Analogues: An Evaluation of Gene Delivery Comparing Polymer Architectures, *J. Am. Chem. Soc.*, 2015, **137**(20), 6541–6549.
39 A. M. vanHerk and T. Droge, Nonlinear least squares fitting applied to copolymerization modeling, *Macromol. Theory Simul.*, 1997, **6**(6), 1263–1276.